O–O Activation

DOI: 10.1002/anie.200906749

O_2 Activation and Selective Phenolate *ortho* Hydroxylation by an Unsymmetric Dicopper μ-η¹:η¹-Peroxido Complex**

Isaac Garcia-Bosch, Anna Company, Jonathan R. Frisch, Miquel Torrent-Sucarrat, Mar Cardellach, Ilaria Gamba, Mireia Güell, Luigi Casella, Lawrence Que, Jr.,* Xavi Ribas,* Josep M. Luis,* and Miquel Costas**

Understanding the intimate details of O_2 activation at metal sites is of interest because of the relevance of such reactions in biological and technological processes.[1] Of particular relevance is uncovering basic chemical principles and mechanisms for taming the high oxidizing potential of the O_2 molecule into highly selective oxidative transformations, especially those involving the selective hydroxylation of C–H bonds.

For the particular case of dicopper sites, three basic Cu_2O_2 core structures have been widely described as arising from the interaction of discrete Cu^I complexes and O_2 (Figure 1).[2] Each specific Cu_2O_2 core determines particular spectroscopic and chemical properties:[2b,c] whereas end-on *trans*-$Cu^{II}_2(\mu\text{-}\eta^1\text{:}\eta^1\text{-}O_2)$ species exhibit nucleophilic and basic behavior, side-on $Cu^{II}_2(\mu\text{-}\eta^2\text{:}\eta^2\text{-}O_2)$ and bis-μ-oxido dicopper(III) $(Cu^{III}_2(\mu\text{-}O)_2)$ cores show electrophilic character, and can mediate tyrosinase-like phenolate *ortho*-hydroxylation reactions.[3] The latter reactivity has never been observed for end-on Cu_2O_2 species; therefore its possible biological relevance has been ignored so far.

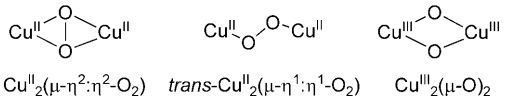

$Cu^{II}_2(\mu\text{-}\eta^2\text{:}\eta^2\text{-}O_2)$ *trans*-$Cu^{II}_2(\mu\text{-}\eta^1\text{:}\eta^1\text{-}O_2)$ $Cu^{III}_2(\mu\text{-}O)_2$

Figure 1.

The rich and subtle chemistry exhibited by Cu_2O_2 cores makes unsymmetric options interesting. Actually, Cu_2O_2 species in systems containing distinct copper sites have been rarely observed.[2b] Herein we describe a novel dicopper complex based on a heptadentate ligand that gives rise to an unsymmetric $N_3Cu^{II}N_4Cu^{II}(\mu\text{-}\eta^1\text{:}\eta^1\text{-}O_2)$ core, which hitherto exhibits reactivity patterns not observed for symmetric analogues. This nonsymmetric peroxide species shows an exquisite selectivity in its oxygen atom transfer reactivity. It performs the selective intermolecular *ortho* hydroxylation of a phenolate, but fails to oxidize many common oxophilic substrates.

Reaction of *m*-Xyl^{N3N4} with $[Cu^I(CH_3CN)_4X]$ ($X = CF_3SO_3$, PF_6, ClO_4) in acetonitrile affords the unsymmetric dinuclear copper(I) complex $[Cu^I_2(m\text{-}Xyl^{N3N4})](X)_2$ (**1**-X; Figure 2). For comparative purposes, $[Cu^I_2(m\text{-}Xyl^{N4N4})](ClO_4)_2$ (**2**-ClO_4) was also prepared. Crystallographic characterization of **1**-CF_3SO_3 reveals that the copper ion bound to the tridentate arm adopts a highly distorted T-shape geometry, whereas the copper ion bound to the tetradentate arm has a distorted trigonal-pyramidal geometry, with structural parameters nearly superimposable with those of the two tetracoordinated copper ions in **2**-ClO_4.[4]

Acetone solutions of **1**-X at −90 °C react with O_2 within seconds to form a red-brown species $[Cu_2(O_2)(m\text{-}Xyl^{N3N4})]^{2+}$ (**1**-O_2), characterized by a visible band at 478 nm ($\varepsilon = 7800\,M^{-1}cm^{-1}$), and a broad shoulder between 575 and 700 nm (Figure 3). The visible spectrum of **1**-O_2 is intermediate between those of Itoh's proposed $Cu^{II}_2(\mu\text{-}\eta^1\text{:}\eta^2\text{-}O_2)$ species[5] and reported $Cu^{II}_2(\mu\text{-}\eta^1\text{:}\eta^1\text{-}O_2)$ complexes.[2b,6] UV/Vis monitoring of this reaction shows an isosbestic point at 414 nm indicating the clean transformation of **1**-CF_3SO_3 into **1**-O_2 without accumulation of any intermediate species. **1**-O_2 is stable for hours at −90 °C, but it decomposes within seconds when warmed to room temperature.

[*] I. Garcia-Bosch, Dr. A. Company,[+] M. Cardellach, Dr. X. Ribas, Dr. M. Costas
Departament de Química, Universitat de Girona
Campus de Montilivi, 17071 Girona, Catalonia (Spain)
E-mail: xavi.ribas@udg.edu
miquel.costas@udg.edu
J. R. Frisch, Prof. L. Que, Jr.
Department of Chemistry and Center for Metals in Biocatalysis
University of Minnesota, 207 Pleasant Street SE
Minneapolis, MN 55545 (USA)
E-mail: larryque@umn.edu
Dr. M. Torrent-Sucarrat
Institut de Química Avançada de Catalunya, IQAC–CSIC
Catalonia (Spain)
Dr. I. Gamba, Prof. L. Casella
Department of General Chemistry, University of Pavia
27100 Pavia (Italy)
E-mail: bioinorg@unipv.it
Dr. M. Güell, Dr. J. M. Luis
Institut de Química Computacional, Universitat de Girona
Catalonia (Spain)
E-mail: josepm.luis@udg.edu
josepm.luis@udg.edu
[+] Present address:
Institut Chemie, Technische Universität Berlin (Germany)

[**] This work was supported financially by MCYT of Spain (projects CTQ2006-05367/BQU and CTQ2009-08464/BQU to M.C.), by the U.S. NIH (grant GM38767 to L.Q.), and by the Italian MIUR (Prin project to L.L.). I.G.B and A.C. thank MICINN for PhD grants. M.T.-S. thanks the CSIC for the JAE-DOC contract. We thank STR-UdG for technical support. M.C. also thanks the Generalitat Catalunya for an ICREA-Academia award and for project 2009 SGR-637.

Supporting information for this article is available on the WWW under http://dx.doi.org/10.1002/anie.200906749.

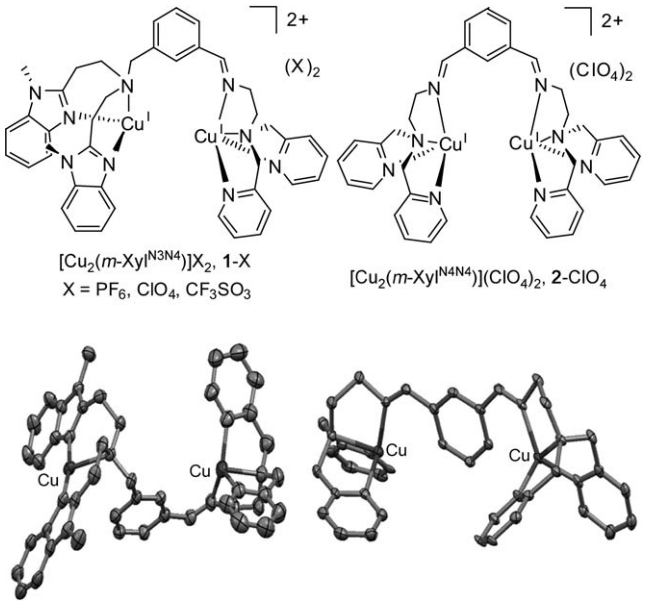

Figure 2. Top: Chemical diagram of **1**-X (left) and **2**-ClO_4 (right). Bottom: Ellipsoid diagrams (30% probability) of the cationic parts of **1**-CF_3SO_3 (left) and **2**-ClO_4 (right). H atoms were omitted for clarity.

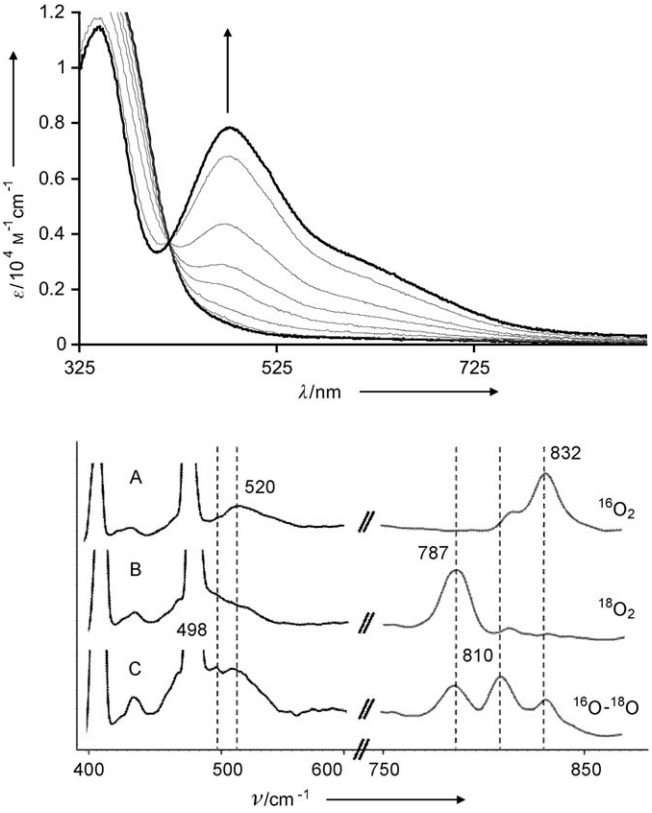

Figure 3. Top: UV/Vis spectra for the reaction of **1**-CF_3SO_3 with O_2 in acetone at −90 °C to form **1**-O_2. Bottom: Resonance Raman spectra (λ_{ex} = 488 nm) of frozen acetone solutions of **1**-O_2 from $^{16}O_2$ (A), $^{18}O_2$ (B), and $^{18}O^{16}O$ (C).

To gain insight into the peroxido binding mode of **1**-O_2, resonance Raman spectra of frozen samples of **1**-O_2 were obtained. Laser excitation at 488 nm (Figure 3 bottom, insets A and B) gives rise to two resonance-enhanced peaks at 832 and 520 cm^{-1} [$\Delta^{18}O_2$-$^{16}O_2$ = 45 and 22 cm^{-1}, respectively], characteristic of O–O and Cu–O stretching vibrations of an end-on $Cu^{II}_2(\mu\text{-}\eta^1\text{:}\eta^1\text{-}O_2)$ species.[2b] Excitation profiles indicate that the two vibrations are in resonance with the lower energy band, and no features resulting from a $Cu^{II}_2(\mu\text{-}\eta^2\text{:}\eta^2\text{-}O_2)$ species were observed. Experiments with mixed labeled O_2 (Figure 3 bottom, inset C) showed a ν(O–O) region with three isotopomeric peaks at frequencies that suggest insensitivity of the bound O_2 to the unsymmetrical nature of the ligand.[7]

In contrast, symmetric complex **2**-ClO_4 reacts at −90 °C in acetone to form a different metastable purple species, **2**-O_2, which is characterized by two intense UV/Vis bands at λ_{max} = 500 nm (ε = 5000 $M^{-1}cm^{-1}$) and 635 nm (ε = 3300 $M^{-1}cm^{-1}$), typical of an end-on *trans*-$Cu^{II}_2(\mu\text{-}\eta^1\text{:}\eta^1\text{:}O_2)$ species.[2b] The O_2-binding mode was confirmed by the resonance Raman spectra of a frozen **2**-O_2 solution, collected with laser excitation at 488 nm (see the Supporting Information), which shows a characteristic resonance-enhanced ν(O–O) band at 826 cm^{-1} [$\Delta^{18}O_2$-$^{16}O_2$ = 44 cm^{-1}]. The fact that both **1**-O_2 and **2**-O_2 give rise to ν(O–O) features of nearly the same frequency strongly suggests that the dioxygen moiety is bound in the same fashion in the two complexes. Because of the high energy of the ν(O–O) stretching frequency,[2b] and because a $\mu\text{-}\eta^1\text{:}\eta^2\text{-}O_2$ binding mode is unlikely for **2**-O_2,[8] we favor a $\mu\text{-}\eta^1\text{:}\eta^1\text{-}O_2$ mode for both O_2 adducts.

The reactivities of **1**-O_2 and **2**-O_2 with different substrates were explored (Schemes 1 and 2). **1**-O_2 and **2**-O_2 rapidly and quantitatively react with CF_3CO_2H releasing H_2O_2 (99% yield, see the Supporting Information). Titration experiments reveal that both reactions are complete with 1 equivalent of H^+ (per Cu), and no other intermediate species are detected when substoichiometric amounts of H^+ are added. **1**-O_2 and **2**-O_2 react neither with thioanisole, styrene, triphenylmethane, nor with electron donors such as ferrocene. Thermal decomposition of **1**-O_2, by warming up acetone solutions to room temperature, in the presence of large excess of toluene (1000 equiv), did not cause toluene oxidation.[9] The addition of PPh_3 (10 equiv) to **1**-O_2 and **2**-O_2 at −90 °C induces fast O_2 release ($t_{1/2} \approx 5$ min) without formation of $OPPh_3$.[10] In sum, all the above observations suggest that **1**-O_2 and **2**-O_2 are not electrophilic oxidants, and typically react like other end-on *trans*-$Cu^{II}_2(\mu\text{-}\eta^1\text{:}\eta^1\text{-}O_2)$ complexes.[11]

However, substantial differences arise when the reactions of **1**-O_2 and **2**-O_2 with benzaldehydes are studied. **2**-O_2 reacts with benzaldehydes to generate the corresponding benzoic acids in quantitative yields. Kinetic analyses of the reactions were performed by using UV/Vis methods to monitor the decay of the spectral features of **2**-O_2. The **2**-O_2 decay rate can be fitted to single exponential processes, and the measured k_{obs} values are linearly dependent on substrate concentration (see the Supporting Information). Reaction of **2**-O_2 against a series of *para*-substituted benzaldehydes was studied and the corresponding decay rate constants were extracted by using UV/Vis methods to monitor the reactions. Plotting the decay rate of **2**-O_2 against the corresponding Hammett substituent constants (σ^+) affords a linear correlation which gives a ρ value of 1.4 (R^2 = 0.98, see the Supporting Information), consistent with a nucleophilic oxidizing species that attacks

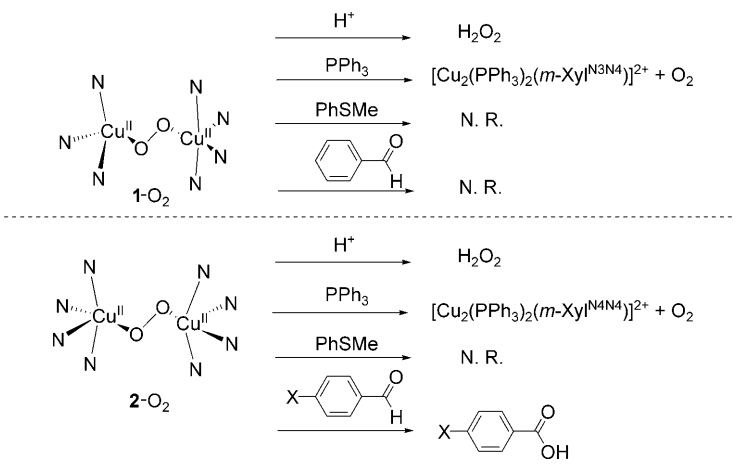

Scheme 1. Schematic representation of selected reactivity exhibited by **1**-O_2 and **2**-O_2. (N.R. = no reaction).

the carbonyl moiety. In contrast, **1**-O_2 fails to react with benzaldehyde. Thus we conclude that **1**-O_2 is unreactive in oxygen atom transfer reactions to common substrates which are either electrophilic or nucleophilic in nature.

Strikingly, addition of *p*-Cl-C_6H_4ONa (3 equiv, Scheme 2) to a solution of **1**-O_2 at −90 °C causes rapid conversion into a short-lived ($t_{1/2} \approx 1$ min) yellow-brown species $\mathbf{3^{Cl}}$ ($\lambda_{max} =$ 470 nm, $\varepsilon > 6000\,M^{-1}cm^{-1}$, see the Supporting Information). The resemblance in the UV/Vis spectral features of **1**-O_2 and $\mathbf{3^{Cl}}$ strongly suggests that the $Cu^{II}_2(\mu\text{-}\eta^1\text{:}\eta^1\text{-}O_2)$ core is retained, but the instability of $\mathbf{3^{Cl}}$ has thus far precluded its Raman characterization. Surprisingly, after complete decomposition of the $\mathbf{3^{Cl}}$ species, acidic work-up and subsequent HPLC/MS analyses show the formation of *p*-chlorocatechol in 39 % yield with respect to **1**-O_2. Similar addition of *p*-chlorophenolate to **2**-O_2 causes fast bleaching of its spectral features, without accumulation of any intermediate species, and without any sign of phenolate *ortho* hydroxylation.

Kinetic analysis indicates that the decay of $\mathbf{3^{Cl}}$ is a first-order process. The analogous species $\mathbf{3^X}$ (X = F, Me, H, and OMe) were generated by the addition of 3 equivalents of *p*-X-C_6H_4ONa to **1**-O_2 at −90 °C in acetone, and their corresponding UV/Vis decay rates were fitted to a single exponential function by nonlinear regression methods. Product analysis after $\mathbf{3^X}$ (X = F, Me, H, and OMe) decomposition reveals that the corresponding catechol is formed in 34 %, 34 %, 36 %, and 14 % yields, respectively. A Hammett plot (log (k_{obs}) for $\mathbf{3^X}$ versus σ^+) affords a linear correlation which gives a ρ value of −0.6 ($R^2 = 0.98$, see the Supporting Information), consistent with an electrophilic oxidizing species that attacks the aromatic ring in the rate-determining step of the reactions. In line with this reactivity, no catechol product was formed when electron-poor phenolates (X = CN, NO_2, and CO_2Me) were used as substrates. In contrast, substrate hydroxylation does not appear to be only determined by the electron-releasing nature of the substrate because the electron-rich, sterically more demanding 2,4-di-*tert*-butylcatecholate was neither hydroxylated nor oxidized to the corresponding diphenol coupled product. We conclude that hydroxylation occurs exclusively for non-electron-poor, sterically unhindered phenolate substrates. Furthermore **1**-O_2 differs from any other $Cu^{II}_2(\mu\text{-}\eta^1\text{:}\eta^1\text{-}O_2)$ intermediate in its capacity to carry out electrophilic arene hydroxylation.[2c] We propose that the difference in the reactivity of **1**-O_2 and any previously reported end-on $Cu^{II}_2(\mu\text{-}\eta^1\text{:}\eta^1\text{-}O_2)$ species (including **2**-O_2) stems from the possibility that phenolate can initially bind at the N_3Cu site, as proposed in a symmetric *m*-xylyl-bridged bis-tridentate $Cu^{II}_2(\mu\text{-}\eta^2\text{:}\eta^2\text{-}O_2)$ system.[3b] Indeed, in the present example, the substrate binding event can be understood as playing a selective peroxide-activation role, since **1**-O_2 by itself lacks oxygen atom transfer reactivity.

The selective oxygen atom transfer reactivity exhibited by **1**-O_2 was additionally substantiated by DFT computational methods.[12] The computed structure of **1**-O_2 (see the Supporting Information) reveals a $Cu^{II}_2(\mu\text{-}\eta^1\text{:}\eta^1\text{-}O_2)$ complex with a Cu···Cu distance of 4.31 Å and structural parameters in good agreement with a crystallographically characterized example.[13] We have also found that the $Cu^{III}_2(\mu\text{-}O)_2$ isomer is 36.8 kcal mol^{-1} higher in energy.[12] In addition, attempts to perform geometry optimizations on side-on $Cu^{II}_2(\mu\text{-}\eta^2\text{:}\eta^2\text{-}O_2)$ isomeric cores proved unsuccessful.[14] Therefore, consistent with the experimental observations, the end-on $Cu^{II}_2(\mu\text{-}\eta^1\text{:}\eta^1\text{-}O_2)$ is the most stable species.[14–16] Phenolate binding to **1**-O_2 retains the $Cu^{II}_2(\mu\text{-}\eta^1\text{:}\eta^1\text{-}O_2)$ core as the most stable isomer (in agreement with our formulation of $\mathbf{3^X}$ based on its UV/Vis spectrum), and causes an elongation of the Cu···Cu distance up to 4.50 Å. Interestingly, the phenolate π system is adjacent to the peroxide oxygen atom bound to the other Cu in $\mathbf{3^{Me}}$ (Figure 4), offering a plausible pathway for a σ* electrophilic attack of the peroxide moiety on the aromatic ring.[17] Most remarkably, the computed activation barrier for this reaction is only 14.7 kcal mol^{-1}, and no intermediates regarding the isomerization to side-on $Cu^{II}_2(\mu\text{-}\eta^2\text{:}\eta^2\text{-}O_2)$ or $Cu^{III}_2(\mu\text{-}O)_2$ cores are found along this attack, thereby strongly suggesting that the *trans* end-on peroxido core is a competent species for executing the aromatic C–H hydroxylation event.[12]

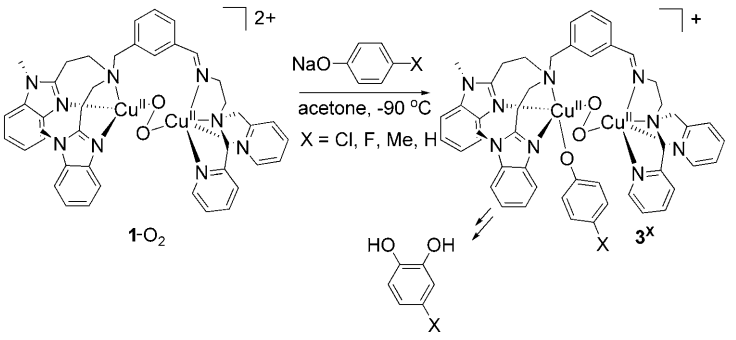

Scheme 2. Reaction of **1**-O_2 with the sodium salt of *para*-substituted phenolate.

In conclusion, our study of O_2 activation at a novel asymmetric dicopper complex **1**-O_2 has hitherto uncovered reactivity patterns thus far not observed for symmetric analogues. **1**-O_2 is basically unreactive in oxygen atom transfer reactions. However, it has an available coordination site that selectively binds phenolate and mediates its *ortho* hydroxylation, therefore functionally mimicking tyrosinase through

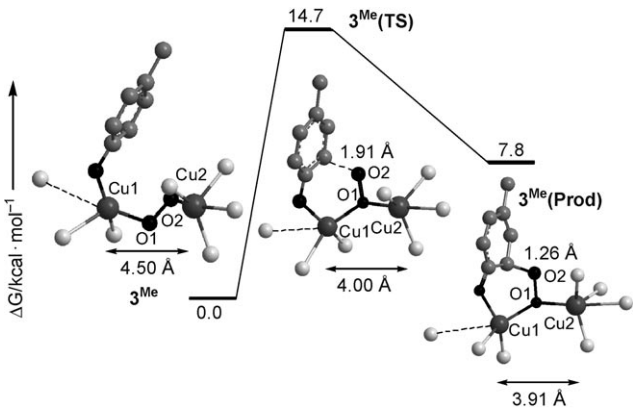

Figure 4. Stationary points along the reaction pathway of the *ortho* hydroxylation of *para*-methyl phenolate into 4-methyl catechol from $\mathbf{3}^{Me}$.

a unique pathway. Furthermore, coordination of the phenolate substrate turns on the unprecedented electrophilic reactivity of the asymmetric end-on *trans*-peroxido core. The combined experimental and computational evidence indicate that the *ortho* hydroxylation of a phenolate by a Cu_2O_2 species can occur by adjacent binding of phenolate and O_2 at a common N_3Cu site without requiring the peroxido to be side-on bound, thus offering a conceptually new understanding of O_2 activation at dicopper sites.

Experimental Section

See the Supporting Information for the full experimental details for the synthesis, spectroscopic, and crystallographic characterization of **1**-X (X = CF_3SO_3, PF_6, ClO_4) and **2**-ClO_4, the experimental procedures for the generation, characterization, and reactivity studies of **1**-O_2 and **2**-O_2, and the computational details on the DFT calculations.

Received: November 30, 2009
Published online: February 28, 2010

Keywords: bioinorganic chemistry · dioxygen ligands · O—O activation · oxidation

[1] a) For an special issue on dioxygen activation by metalloenzymes and models, see W. Nam, *Acc. Chem. Res.* **2007**, *40*, Issue 7; b) T. Punniyamurthy, S. Velusamy, J. Iqbal, *Chem. Rev.* **2005**, *105*, 2329 – 2364; c) D. T. Sawyer, *Oxygen Chemistry*, Oxford University Press, Oxford, **1991**.

[2] a) S. Itoh in *Comprehensive Coordination Chemistry II*, *Vol. 8* (Eds.: L. Que, Jr., W. B. Tolman), Elsevier, Amsterdam, **2004**, pp. 369 – 393; b) L. M. Mirica, X. Ottenwaelder, T. D. P. Stack, *Chem. Rev.* **2004**, *104*, 1013 – 1046; c) E. A. Lewis, W. B. Tolman, *Chem. Rev.* **2004**, *104*, 1047 – 1076; d) L. Q. Hatcher, K. D. Karlin, *J. Biol. Inorg. Chem.* **2004**, *9*, 669 – 683; e) G. Battaini, A. Granata, E. Monzani, M. Gullotti, L. Casella, *Adv. Inorg. Chem.* **2006**, *58*, 185 – 233.

[3] a) S. Itoh, H. Kumei, M. Taki, S. Nagatomo, T. Kitagawa, S. Fukuzumi, *J. Am. Chem. Soc.* **2001**, *123*, 6708 – 6709; b) S. Palavicini, A. Granata, E. Monzani, L. Casella, *J. Am. Chem. Soc.* **2005**, *127*, 18031 – 18036; c) L. M. Mirica, M. Vance, D. J. Rudd, B. Hedman, K. O. Hodgson, E. I. Solomon, T. D. P. Stack, *Science* **2005**, *308*, 1890 – 1892; d) A. Company, S. Palavicini, I. Garcia-Bosch, R. Mas-Ballesté, L. Que, Jr., E. V. Rybak-Akimova, L. Casella, X. Ribas, M. Costas, *Chem. Eur. J.* **2008**, *14*, 3535 – 3538; e) S. Herres-Pawlis, P. Verma, R. Haase, P. Kang, C. T. Lyons, E. C. Wasinger, U. Flörke, G. Henkel, T. D. P. Stack, *J. Am. Chem. Soc.* **2009**, *131*, 1154 – 1169.

[4] CCDC 755536 (**1**CF_3SO_3) and 755537 (**2**ClO_4) contain the supplementary crystallographic data for this paper. These data can be obtained free of charge from The Cambridge Crystallographic Data Centre via www.ccdc.cam.ac.uk/data_request/cif.

[5] Y. Tachi, K. Aita, S. Teramae, F. Tani, Y. Naruta, S. Fukuzumi, S. Itoh, *Inorg. Chem.* **2004**, *43*, 4558 – 4560.

[6] H. Börzel, P. Comba, K. S. Hagen, M. Kerscher, H. Pritzkow, M. Schatz, S. Schindler, O. Walter, *Inorg. Chem.* **2002**, *41*, 5440 – 5452.

[7] The CuO_2 local symmetry cannot necessarily be established by isotopomeric O_2 fragments. C. R. Kinsinger, B. F. Gherman, L. Gagliardi, C. J. Cramer, *J. Biol. Inorg. Chem.* **2005**, *10*, 778 – 789.

[8] Bis-tetradentate ligands most often give rise to μ-η^1-η^1 isomers: see [2b] and references within.

[9] Aliphatic C—H oxidation of toluene mediated by $Cu^{II}_2(\mu\text{-}\eta^1\text{:}\eta^1\text{-}O_2)$ species has been recently reported: a) H. R. Lucas, L. Li, A. A. Narducci Sarjeant, M. A. Vance, E. I. Solomon, K. D. Karlin, *J. Am. Chem. Soc.* **2009**, *131*, 3230 – 3245; b) C. Würtele, O. Sander, V. Lutz, T. Waitz, F. Tuczek, S. Schindler, *J. Am. Chem. Soc.* **2009**, *131*, 7544 – 7545.

[10] ^1H and ^{31}P NMR spectra of the final mixture are identical to those observed after mixing **1**ClO_4 and 10 equivalents PPh_3 in CD_3CN under argon. See the Supporting Information for details.

[11] P. P. Paul, Z. Tyeklar, R. R. Jacobson, K. D. Karlin, *J. Am. Chem. Soc.* **1991**, *113*, 5322 – 5332.

[12] DFT geometries were optimized at the B3LYP level in junction of the SDD basis set and associated ECP for Cu, 6-311G(d) basis set for the atoms bond to Cu, and 6-31G basis set for the other atoms, as implemented in the Gaussian 03 program (see the Supporting Information). The energies were additionally refined by single-point calculations using cc-pVTZ basis set for Cu and the atoms bond to Cu, and cc-pVDZ basis set for the other atoms. Final free energies given in this work include energies computed at the B3LYP/cc-pVTZ&cc-pVDZ//B3LYP/SDD&6-311G(d)&6-31G level of theory together with zero-point energies, thermal corrections, and entropy calculated at the B3LYP/SDD&6-311G(d)&6-31G level. The same qualitative results were also obtained with the BLYP and OPBE methods.

[13] Z. Tyeklár, R. R. Jacobson, N. Wei, N. N. Murthy, J. Zubieta, K. D. Karlin, *J. Am. Chem. Soc.* **1993**, *115*, 2677 – 2689.

[14] $Cu^{II}_2(\mu\text{-}\eta^1\text{:}\eta^1\text{-}O_2)$ to $Cu^{II}_2(\mu\text{-}\eta^2\text{:}\eta^2\text{-}O_2)$isomerization is precedented; a) J. A. Halfen, V. G. Young, Jr., W. B. Tolman, *J. Am. Chem. Soc.* **1996**, *118*, 10920 – 10921; b) B. Jung, K. D. Karlin, A. D. Zuberbühler, *J. Am. Chem. Soc.* **1996**, *118*, 3763 – 3764.

[15] For recent computational studies evaluating $Cu^{II}_2(\mu\text{-}\eta^1\text{:}\eta^2\text{-}O_2)$ species as arene hydroxylating species, see: a) P. E. M. Siegbahn, *J. Biol. Inorg. Chem.* **2003**, *8*, 567 – 576; b) O. Sander, A. Henß, C. Näther, C. C. Würtele, M. C. Holthausen, S. Schindler, F. Tuczek, *Chem. Eur. J.* **2008**, *14*, 9714 – 9729; c) T. Inoue, Y. Shiota, K. Yoshizawa, *J. Am. Chem. Soc.* **2008**, *130*, 16890 – 16897.

[16] Because of the energy proximity of the asymmetric $Cu^{II}_2(\mu\text{-}\eta^1\text{:}\eta^2\text{-}O_2)$ species (+1 kcal mol^{-1}), we have also considered its ability to bind phenolate, and found that upon phenolate coordination the species also converts into a $Cu^{II}_2(\mu\text{-}\eta^1\text{:}\eta^1\text{-}O_2)$ core.

[17] H. Decker, R. Dillinger, F. Tuczek, *Angew. Chem.* **2000**, *112*, 1656 – 1660; *Angew. Chem. Int. Ed.* **2000**, *39*, 1591 – 1595.

